CHAPTER 1
Introduction

1.1 Light Microscopy

The light microscope is one of the significant inventions in the history of humankind that, along with the telescope, played a central role in the Scientific Revolution, which started around 1600.[1] Despite its long history, of more than four centuries, the microscopy field has continuously expanded, covering a growing number of methods.[2] Much of the effort in the field has been devoted to improving two main properties of the microscopic image: *resolution* and *contrast*.

In terms of resolution, Abbe showed in 1873 that the ultimate, theoretical limit for far-field imaging is, essentially, half the wavelength of light.[3] Since then, researchers mainly have worked on approaching this limit (by aberration correction, etc.) rather than exceeding it. The first superresolution optical imaging occurred much more recently, by employing evanescent rather than propagating waves.[4] Remarkably, in the past decade or so, several methods have been developed to exceed the diffraction barrier in *far-field* fluorescence microscopy. Thus, techniques such as STED (stimulated emission depletion),[5–7] (f)PALM (fluorescence photoactivation localization microscopy),[8–14] STORM (stochastic optical reconstruction microscopy),[15–17] and structured illumination[18] represent a departure from the diffraction-limited imaging formulated by Abbe.[3]

There are two main kinds of contrast: *endogenous* and *exogenous*. The endogenous (intrinsic) contrast is generated by revealing the structures as they appear naturally. This challenge is typically addressed via *optical* solutions, i.e., by exploiting the phenomenon of light-matter interaction. On the other hand, exogenous contrast is produced by attaching a contrast agent (e.g., stain, fluorescent dye) to the structure of interest. A remarkable development in fluorescence microscopy is the technology based on green fluorescent protein (GFP).[19] In this case, live cells are genetically modified to express GFP, a protein purified from jellyfish, which essentially converts the exogenous into endogenous contrast generation. Deep-tissue imaging is also a contrast problem, which is addressed via techniques such as

confocal microscopy, nonlinear microscopy, and optical coherence tomography.

1.2 Quantitative-Phase Imaging (QPI)

The great obstacle in generating intrinsic contrast from optically thin specimens (including live cells) is that, generally, they do not absorb or scatter light significantly, i.e., they are transparent, or *phase objects*. In his theory, Abbe described image formation as an interference phenomenon,[3] opening the door for formulating the problem of contrast precisely as in interferometry. Exploiting this concept, in the 1930s Zernike developed phase-contrast microscopy (PCM), in which the contrast of the interferogram generated by the scattered and unscattered light (i.e., the contrast of the image) is enhanced by shifting their relative phase by a quarter wavelength and further matching their relative power.[20,21] PCM represents a major advance in intrinsic contrast imaging, as it reveals inner details of transparent structures without staining or tagging. However, the resulting phase-contrast image is an *intensity* distribution, in which the *phase* information is coupled nonlinearly and cannot be retrieved *quantitatively*.

In the 1940s, Gabor understood the significance of the phase information and proposed *holography* as an approach to exploit it for imaging purposes.[22] It became clear that knowing both the amplitude and phase of the field allows imaging to be treated as transmission of information, akin to radio communication.[23]

QPI essentially combines the pioneering ideas of Abbe, Zernike, and Gabor (Fig. 1.1). The resulting image is a map of pathlength shifts associated with the specimen. Of course, this image contains information about both the local thickness and refractive index of the structure, which makes the decoupling of their respective contributions

Figure 1.1 Pioneers of coherent light microscopy.

challenging. At the same time, recent work shows that QPI provides a powerful means to study dynamics associated with both thickness and refractive index fluctuations. Remarkably, the quantitative-phase map associated with a live cell reports on the cell's dry mass density, i.e., its non-aqueous content.[24,25] Thus, QPI has the ability to quantify cell growth with *femtogram* sensitivity and without contact.[26]

1.3 QPI and Multimodal Investigation

From the knowledge of spatially resolved phase distribution, $\phi(x, y)$, various other visualization modalities can be easily obtained by simple numerical calculations. Figure 1.2 shows how, by taking the 1D gradient of a quantitative-phase image, an image similar to that of differential interference contrast (DIC) microscopy is obtained (Fig. 1.2*b*). In QPI, we have the additional flexibility of numerically removing the "shadow artifact" associated with DIC images. This artifact is due to the first-order derivative-changing sign across an edge and can be easily eliminated by taking the modulus of the gradient (Fig. 1.2*c*). Further, the Laplacian of the phase image reveals fine details (high-frequency content) from the specimen (Fig. 1.2*d*).

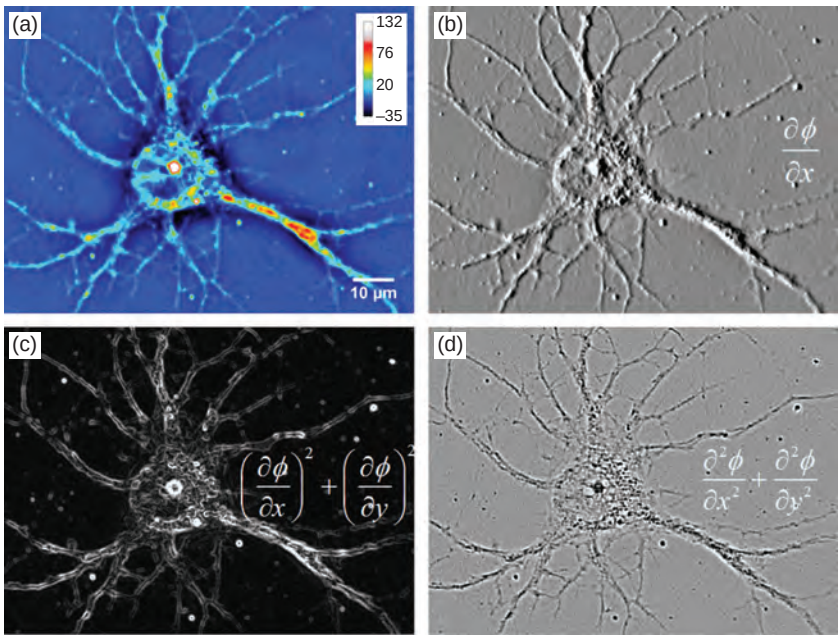

Figure 1.2 (*a*) QPI of a neuron (colorbar shows pathlength in nanometer). (*b*) Synthetic DIC image obtained by taking a 1D derivative of *a*. (*c*) Image obtained by taking the modulus squared of the gradient associated with *a*. (*d*) Image obtained by taking the Laplacian of *a*.

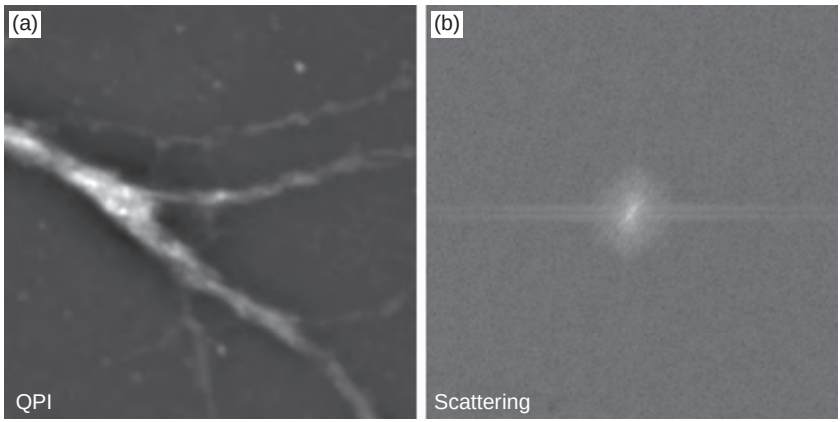

Figure 1.3 Fourier transform light scattering. (*a*) QPI of dendrites; (*b*) scattering map from dendrites in *a*.

Perhaps one of the most striking features of QPI is that it can generate *light-scattering* data with extreme sensitivity. This happens because full knowledge of the complex (i.e., amplitude and phase) field at a given plane (the image plane) allows us to infer the field distribution at any other plane, including in the far zone. In other words, the image and scattering fields are simply Fourier transforms of each other; this relationship does not hold in intensity. Figure 1.3 shows the QPI of a dendritic structure (lower-right corner of Fig. 1.2*a*) and its corresponding scattering map obtained by taking the Fourier transform of the image field. This approach, called Fourier transform light scattering (FTLS) is much more sensitive than common, goniometer-based angular scattering because the measurement takes place at the image plane, where the optical field is most uniform. As a result, FTLS can render with ease scattering properties of minute subcellular structures which is unprecedented.

1.4 Nanoscale and Three-Dimensional Imaging

Sometimes, some confusion emerges regarding QPI, especially in the context of *nanoscale* and *3D imaging*. Here we briefly address these two issues.

First, it is clear that QPI provides sensitivity to spatial and temporal pathlength changes down to the *nanoscale*. This has been exploited, for example, in studies of red blood cell fluctuations and topography of nanostructures. Figure 1.4 illustrates the nanoscale sensitivity to pathlength changes caused by transport along a neuron dendrite. However, this *sensitivity* should not be referred to as axial *resolution*. Nanometer resolution, or resolving power, would describe the ability

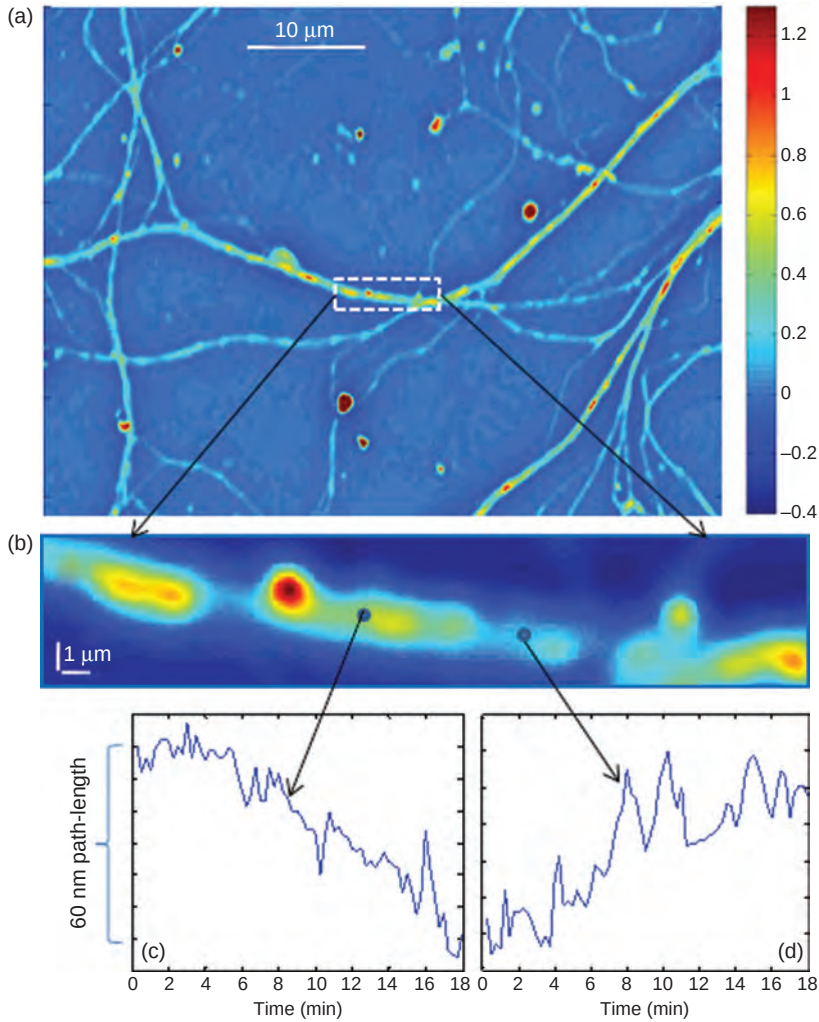

Figure 1.4 (*a*) QPI image of live neuronal processes. (*b*) The magnified region indicated in *a*. (*c* and *d*) Nanoscale temporal sensitivity to pathlength fluctuations associated with the respective points in *b*.

of QPI to resolve two objects separated axially by 1 nm. Of course, this is impossible, as it would violate the uncertainty principle.

Second, QPI images are occasionally represented as surface plots of the form in Fig. 1.5*a*. Perhaps because these plots contain three axes, (ϕ, x, y), sometimes QPI is erroneously referred to as *3D imaging*. Note that 3D imaging, or *tomography*, means resolving a physical property of the object (in this case refractive index, n) in all three dimensions. Rrepresenting these tomographic data requires four axes

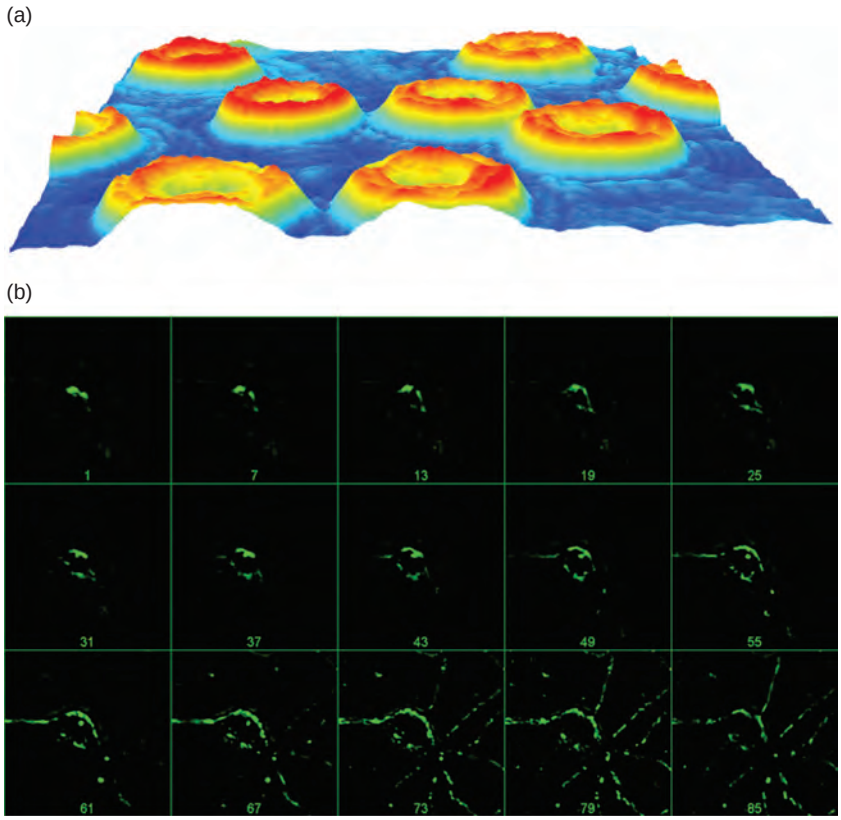

Figure 1.5 (*a*) Surface plot representation of quantitative-phase image, ϕ (*x*, *y*). (*b*) Montage representation of a tomogram, *n* (*x*, *y*, *z*). Images 1 to 85 represent different slices along *z*.

(*n*, *x*, *y*, *z*), which means that in a plot only certain sections or projections of the data can be represented (Fig. 1.5*b*). While QPI can be used to perform tomography (see Chap. 14), this operation requires acquisition of images vs. an additional dimension, e.g., wavelength, sample rotation angle, or sample axial position.

References

1. R. P. Carlisle, *Scientific American Inventions and Discoveries: All the Milestones in Ingenuity—from the Discovery of Fire to the Invention of the Microwave Oven* (John Wiley & Sons, Hoboken, N, 2004).
2. Milestones in light microscopy, *Nat Cell Biol*, 11, 1165–1165 (2009).
3. E. Abbe, Beiträge zur Theorie des Mikroskops und der mikroskopischen Wahrnehmung, *Arch. Mikrosk. Anat.*, 9, 431 (1873).
4. E. Betzig, J. K. Trautman, T. D. Harris, J. S. Weiner and R. L. Kostelak, Breaking the diffraction barrier-optical microscopy on a nanometric scale, *Science*, 251, 1468–1470 (1991).

5. R. Schmidt, C. A. Wurm, S. Jakobs, J. Engelhardt, A. Egner and S. W. Hell, Spherical nanosized focal spot unravels the interior of cells, *Nature Methods*, 5, 539–544 (2008).
6. J. Folling, M. Bossi, H. Bock, R. Medda, C. A. Wurm, B. Hein, S. Jakobs, C. Eggeling and S. W. Hell, Fluorescence nanoscopy by ground-state depletion and single-molecule return, *Nature Methods*, 5, 943–945 (2008).
7. K. I. Willig, R. R. Kellner, R. Medda, B. Hein, S. Jakobs and S. W. Hell, Nanoscale resolution in GFP-based microscopy, *Nature Methods*, 3, 721–723 (2006).
8. H. Shroff, C. G. Galbraith, J. A. Galbraith and E. Betzig, Live-cell photoactivated localization microscopy of nanoscale adhesion dynamics, *Nature Methods*, 5, 417–423 (2008).
9. S. Manley, J. M. Gillette, G. H. Patterson, H. Shroff, H. F. Hess, E. Betzig and J. Lippincott-Schwartz, High-density mapping of single-molecule trajectories with photoactivated localization microscopy, *Nature Methods*, 5, 155–157 (2008).
10. H. Shroff, C. G. Galbraith, J. A. Galbraith, H. White, J. Gillette, S. Olenych, M. W. Davidson and E. Betzig, Dual-color superresolution imaging of genetically expressed probes within individual adhesion complexes, *Proceedings of the National Academy of Sciences of the United States of America*, 104, 20308–20313 (2007).
11. E. Betzig, G. H. Patterson, R. Sougrat, O. W. Lindwasser, S. Olenych, J. S. Bonifacino, M. W. Davidson, J. Lippincott-Schwartz and H. F. Hess, Imaging intracellular fluorescent proteins at nanometer resolution, *Science*, 313, 1642–1645 (2006).
12. T. J. Gould, M. S. Gunewardene, M. V. Gudheti, V. V. Verkhusha, S. R. Yin, J. A. Gosse and S. T. Hess, Nanoscale imaging of molecular positions and anisotropies, *Nature Methods*, 5, 1027–1030 (2008).
13. S. T. Hess, T. P. K. Girirajan and M. D. Mason, Ultra-high resolution imaging by fluorescence photoactivation localization microscopy, *Biophysical Journal*, 91, 4258–4272 (2006).
14. M. F. Juette, T. J. Gould, M. D. Lessard, M. J. Mlodzianoski, B. S. Nagpure, B. T. Bennett, S. T. Hess and J. Bewersdorf, Three-dimensional sub-100 nm resolution fluorescence microscopy of thick samples, *Nature Methods*, 5, 527–529 (2008).
15. B. Huang, W. Q. Wang, M. Bates and X. W. Zhuang, Three-dimensional super-resolution imaging by stochastic optical reconstruction microscopy, *Science*, 319, 810–813 (2008).
16. M. Bates, B. Huang, G. T. Dempsey and X. W. Zhuang, Multicolor super-resolution imaging with photo-switchable fluorescent probes, *Science*, 317, 1749–1753 (2007).
17. M. J. Rust, M. Bates and X. W. Zhuang, Sub-diffraction-limit imaging by stochastic optical reconstruction microscopy (STORM), *Nature Methods*, 3, 793–795 (2006).
18. M. G. L. Gustafsson, Nonlinear structured-illumination microscopy: Wide-field fluorescence imaging with theoretically unlimited resolution, *Proceedings of the National Academy of Sciences of the United States of America*, 102, 13081–13086 (2005).
19. R. Y. Tsien, The green fluorescent protein, *Annual Review of Biochemistry*, 67, 509–544 (1998).
20. F. Zernike, Phase contrast, a new method for the microscopic observation of transparent objects, Part 2, *Physica*, 9, 974–986 (1942).
21. F. Zernike, Phase contrast, a new method for the microscopic observation of transparent objects, Part 1, *Physica*, 9, 686–698 (1942).
22. D. Gabor, A new microscopic principle, *Nature*, 161, 777 (1948).
23. D. Gabor, theory of communicaton, *J. Inst. Electr. Eng.*, 93, 329 (1946).
24. H. G. Davies and M. H. Wilkins, Interference microscopy and mass determination, *Nature*, 169, 541 (1952).
25. R. Barer, Interference microscopy and mass determination, *Nature*, 169, 366–367 (1952).
26. G. Popescu, Y. Park, N. Lue, C. Best-Popescu, L. Deflores, R. R. Dasari, M. S. Feld and K. Badizadegan, Optical imaging of cell mass and growth dynamics, *Am J Physiol Cell Physiol*, 295, C538–544 (2008).